2012 IEEE/RSJ International Conference on
Intelligent Robots and Systems
October 7-12, 2012. Vilamoura, Algarve, Portugal

Design of Soft Robotic Actuators using Fluid-filled Fiber-Reinforced Elastomeric Enclosures in Parallel Combinations

Joshua Bishop-Moser*, Girish Krishnan*, Charles Kim, and Sridhar Kota

Abstract*— Complex controlled motions, soft human interaction, and minimal moving mass all drive the need for soft robots using fluid filled fiber reinforced elastomer enclosures (FREEs). While a narrow class of FREEs known as McKibben's actuators have been extensively studied, there is a wide unexplored class with complex sets of motion patterns. Combining these actuators in parallel can yield versatile motion patterns resulting in a large overall workspace. Mobility of individual actuators is enforced by inextensibility of fibers and incompressibility of fluids, which in turn drives the net attainable motions. In this paper, we map the mobility of individual FREE actuators to all possible resultant motions that a combination of three sets of actuators arranged in a triangular configuration would undergo. This understanding has resulted in a preliminary design tool that determines individual FREE topologies for a required set of motion patterns. Five case studies that result from this methodology are prototyped and tested for comparison of the predicted and obtained motion directions.

I. Introduction

Fiber Reinforced Elastomeric Enclosures (FREEs) are hollow enclosures made of elastomer surfaces reinforced with a network of fibers. The enclosures typically contain pressurized fluid, which upon interaction with the FREE surface present a wide range of deformation patterns. These structures are ubiquitous in nature [1] from starfishes to octopus tentacles. There is building interest in using FREEs in engineering applications, as they have high power to weight ratio, can be made with inexpensive materials and manufacturing processes, and are safe for human interaction. The commercially available McKibben's actuator [2], or pneumatic air muscle, is an example FREE that contracts when pressurized. A number of researchers have developed robots and devices using these simple FREEs, such as an octopus like manipulator, OctArm, by Trivedi et al. [3] and similar designs described in Greef et al. [4], Trivedi et al. [5], and Webster et al. [6]. These robots and devices exclusively utilize actuation chambers that perform simple motions when inflated, thus limiting the potential wealth of motions soft robots could have.

* These authors have contributed equally towards the work.

Joshua Bishop-Moser is a Graduate Student in the Department of Mechanical Engineering, University of Michigan, Ann Arbor, MI 48109, USA joshbm@umich.edu

Girish Krishnan is a Post-Doctoral Research Assistant in the Department of Mechanical Engineering, University of Michigan, Ann Arbor, MI 48109, USA gikrishn@umich.edu

Charles Kim is an Assistant Professor in the Department of Mechanical Engineering, Bucknell University, Lewisberg, PA 17837, USA charles.kim@bucknell.edu

Sridhar Kota is a Professor in the Department of Mechanical Engineering, University of Michigan, Ann Arbor, MI 48109, USA kota@umich.edu

In this paper, we investigate a parallel combination of a wide class of cylindrical FREEs that can simultaneously provide translation, bending, rotations, and screw motions. Parallel combination provides robust motion, enables independent control of the degrees of freedom and are less influenced by inertia effects. These advantages are resonated in traditional mechanisms by Merlet [7] and compliant mechanisms by Hopkins et al. [8]. Preliminary constraint analysis for a small class of FREEs has been conducted by Hirai et al. [9]. Though Hirai et al. [10] propose combining individual FREEs in parallel, a systematic type synthesis has not been laid out. In this paper, we propose a design methodology that combines three individual classes of FREEs in parallel to obtain complex sets of motion. This is accomplished in the paper by:

1) Determining the geometric relationships that govern the deformation behavior of cylindrical FREEs for all possible fiber orientations (elucidated in Section II).
2) Identifying directions of freedoms, constrains and actuation for these cylindrical FREEs (section III).
3) Determining the mapping of the mobility from single FREE actuators to a parallel combination of three actuators (Section IV).
4) Fabricating and testing five distinct parallel actuator combinations to determine the direction of motion under all actuation permutations (Section V).

II. FREE: Governing Behavior

The deformation behavior of FREEs are governed by the **i.** Inextensibility of fibers, **ii.** Incompressibility of fluids, and **iii.** deformation of the hyperelastic membrane. Some simplifying assumptions about the FREE's geometry and deformation behavior restrict the analysis and conclusions to a certain class of cylindrical FREEs. These are:

1) initial and final geometries are perfect cylinders.
2) The fibers are closely laid with large volume fractions.
3) Fluid is incompressible, and its enclosed volume can be controlled by the user. Thus, there is a one-one relation between fluid volume and FREE deformation.
4) The effect of the elastomer that encloses the fibers and fluids is ignored.

The axial and radial deformation of a cylinder are expressed as stretch ratios λ_1 and λ_2 respectively. Fibers are described as helices with an angle of α and β with respect to the axis of the cylinder (see Fig. 1). θ is the number of rotations of the fiber in radians, and θ^* the rotations after deformation, with the difference describing the cylinder

978-1-4673-1736-8/12/S31.00 ©2012 IEEE

rotation as angle δ. The volume enclosed within the cylinder before deformation is V, and V^* after deformation. Setting

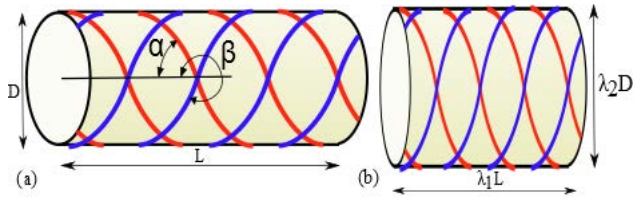

Fig. 1. (a) FREE with 2 sets of helical fibers at angles α and β. (b) Compressed FREE with stretch ratios λ_1 and λ_2.

the fiber length before and after deformation to be equal provides Eq. 1 for a single fiber, with the volume of the fluid enclosed within the cylinder expressed as equations V^*. With two families of helical fibers, the two equations of fiber inextensibility (Eq. 1) can be combined and written as Eqs. 2 and 3.

$$\lambda_1^2(\cos\alpha)^2 + \lambda_2^2(\sin\alpha)^2(\frac{\theta^*}{\theta})^2 = 1 \qquad V^* = \lambda_2^2\lambda_1\pi r^2 l \tag{1}$$

$$\lambda_2 = \frac{\sqrt{1-\cos(\beta)^2\lambda_1^2}\cos(\alpha) - \sqrt{1-\cos(\alpha)^2\lambda_1^2}\cos(\beta)}{\sin(\alpha-\beta)} \tag{2}$$

$$\delta = \frac{l}{r}\frac{\sin(\alpha)\sqrt{1-\lambda_1^2\cos(\beta)^2} - \sin(\beta)\sqrt{1-\lambda_1^2\cos(\alpha)^2}}{\cos(\beta)\sqrt{1-\lambda_1^2\cos(\alpha)^2} - \cos(\alpha)\sqrt{1-\lambda_1^2\cos(\beta)^2}} \tag{3}$$

III. Design Space Spanned by Helical FREEs

To understand the mobility created by these families of fibers, the space of all possible configurations was divided into the 26 regions with each region possessing a different mobility than their adjacent regions. Figure 2(a) shows all these regions, with α and β representing the angle of first and second families of fibers respectively. The $\alpha = \beta$ line signifies degeneration of one family into another. Figure 2(b) shows the 11 mobility directions possible for a single actuator. The regions that are not along an axis are screw motions, and have a mobility that is a specific combination of the motions along the axes. Region (F), for example, has a mobility in which the actuator simultaneously extends and rotates counter clockwise in an interconnected manner.

The deformation of the FREE structures depends on the change in λ_1 and λ_2 with respect to volume change. If the sign of $dV/d\lambda_1$ is positive, axial length is positively correlated with volume change, while a negative value is associated with axial contraction under volumetric expansion. There is a set of fiber angle configurations for which this derivative is zero, implying that no amount of axial expansion or contraction can cause an increase in volume. These set of fiber configurations can be obtained by evaluating $dV/d\lambda_1$ by differentiating Eq. 1 at the undeformed position ($\lambda_1 = 1$) and setting it equal to zero as shown in Eq. 4. These configurations are understood to be locked under actuation. These are plotted in Fig. 2(a) as regions 22, 23, and 26. For most configurations a well-defined relationship exists

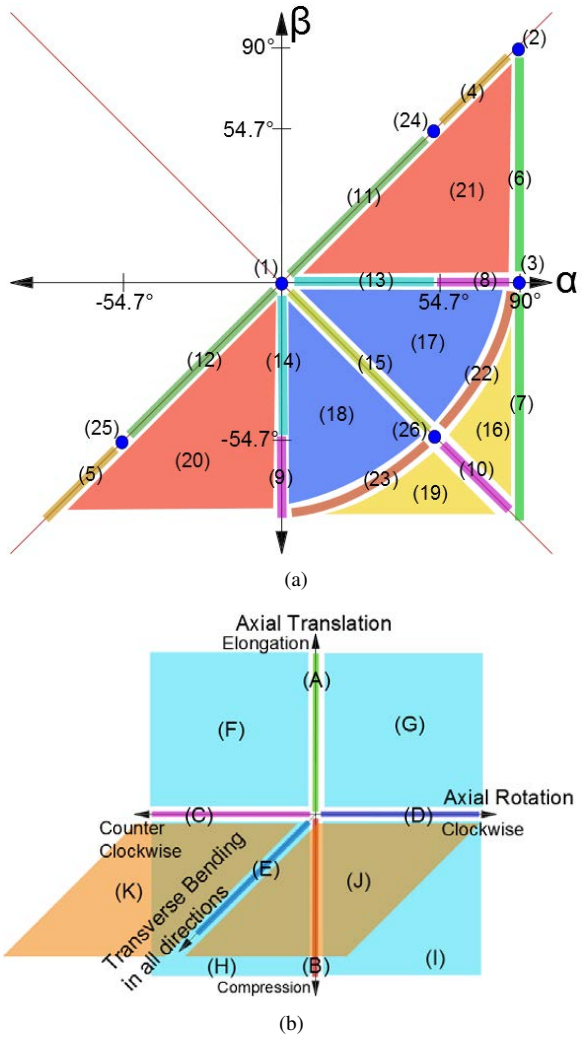

Fig. 2. (a) All 26 actuator types created by 2 families of fibers, with fiber angles α and β respectively. Actuators on the $45°$ line are degenerate cases with a single family of fibers. Each actuator has a different mobility than ones adjacent to itself. (b) All mobility directions possible for single actuators, shown on a 3-dimensional plot with each axis representing a mobility direction. Regions shown in cyan and orange are screw motions.

between the axial stretch and rotation, referred to as the pitch. This implies that the general form of deformation for these geometries is a *screw* motion. For small deformations about its initial configuration, the pitch is defined as Eq. 5.

$$\lim_{\lambda_1\to 1}\frac{dV}{d\lambda_1} = 0 \implies \alpha = \cot^{-1}(\frac{-1}{2\cot(\beta)}) \tag{4}$$

$$p_{norm} = \lim_{\lambda_1\to 1}\frac{ld\lambda_1}{rd\delta} \tag{5}$$

A. Special Points and Regions

While the previous section dealt with configurations with definite relationships between the stretch ratios and rotation, there are some special configurations for which these relationships vanish.

1) $\alpha = 90°$ and $\beta = 0°$ (region 3): Substituting $\lambda_1 = 1$ $\lambda_2 = 1$ in Eq. 3, yields $\delta = 0$.
2) $\alpha = \beta$ (regions 4, 5, 11, 12, 24, 25): Equations 1 and 3 provides two independent variables, λ_1 and δ, whose

relative magnitudes can be arbitrary as long as volume is increases.

3) $\alpha = \beta = 0$ (region 1). $\lambda_1 = 1$, thus volume is expressed just in terms of λ_2.
4) $\alpha = \beta = 90°$ (region 2): $\lambda_2 = 1$ and from Eq. 3, $\delta = 0$. The volume is dependent only on λ_1.

B. Freedom Directions

Inextensibility of fibers and incompressibility of fluids act as constraints against deformation from external forces. For example, configurations with longitudinal fibers ($\alpha = 0°$ or $\lambda_1 = 1$) are constrained against bending. By determining the constraint imparted by each of the motion directions, a matrix mapping the actuator types to their respective mobility directions for both actuation and freedoms shown in Table I is created. "A" indicates a mobility that the actuator will move under increasing volume, while "F" indicates a mobility that the actuator is free to move without changing the volume or extending any fibers.

TABLE I

THE MOBILITY MAPPING FOR ALL SINGLE ACTUATORS. "A" IS AN ACTUATION DIRECTION THAT INCREASES VOLUME; "F" IS A FREEDOM DIRECTION THAT KEEPS VOLUME CONSTANT.

Actuator Type	Mobility Direction (from Fig. 2(b))										
(from Fig. 2(a))	A	B	C	D	E	F	G	H	I	J	K
1	.	F	F	F	F	.	.	.	.	.	.
2	A	.	F	F	F	.	.	.	.	.	.
3	.	.	F	F	.	.	.	.	.	.	.
4	A	.	A	.	F	F	.	.	F	.	.
5	A	.	.	A	F	.	F	F	.	.	.
6	.	.	.	.	F	.	A	.	.	.	.
7	.	.	.	.	F	A	.	.	.	.	.
8	.	.	A	.	.	.	.	.	F	F	.
9	.	.	.	A	.	.	.	F	.	.	F
10	A	.	.	.	F	.	.	.	.	.	.
11	.	A	A	.	F	.	F	F	.	.	.
12	.	A	.	A	F	F	.	.	F	.	.
13	.	A	A	.	.	.	.	F	.	F	.
14	.	A	.	A	.	.	.	.	F	.	F
15	.	A	.	.	F	.	.	F	F	.	.
16	.	.	.	.	F	A	.	.	.	.	.
17	.	.	.	.	F	.	.	A	.	.	.
18	.	.	.	.	F	.	.	.	A	.	.
19	.	.	.	.	F	.	A	.	.	.	.
20	.	.	.	.	F	A	.	.	.	.	.
21	.	.	.	.	F	.	A	.	.	.	.
22	.	.	.	.	F	.	.	.	.	.	.
23	.	.	.	.	F	.	.	.	.	.	.
24	.	.	A	.	F	.	F	.	F	.	.
25	.	.	.	A	F	F	.	F	.	.	.
26	.	.	.	.	F	.	.	.	.	.	.

IV. MOBILITY COUPLING OF PARALLEL FREES

In order to determine the mobility of parallel actuators, the mobility of all constituent elements is combined. This is accomplished by combining the five mobility types that are possible for cylindrical FREEs, with the parallel mobility spanning permutations of these types. These types are axial translation, transverse bending, trans-actuator bending, rotation, and screw coupling, and are shown in Fig. 3. Trans-actuator bending is a coupled transverse motion created by two or more actuators that allows for bending with a neutral axis that is not at the center of one or more actuators. Screw coupling determines if an actuator has a screw mobility which couples rotation to transverse bending or axial translation. These screw mobilities are shown as sections (F) through (K) of Fig. 2(b).

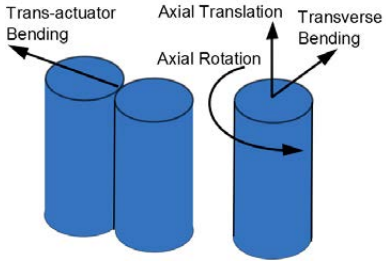

Fig. 3. Fundamental mobility directions for parallel sets of actuators. There is an additional screw motion coupling rotation to translation, transverse bending, or trans-actuator bending.

A. Coupling of Triangular Triplets of Actuators

There are 44 coordinate dependent mobility directions for triangular triplets of actuators. Four of the motions follow a rather simple set of rules:

1) Axial translation is a parallel mobility if and only if all actuators have mobility in axial translation in the parallel mobility direction.
2) Rotation is a parallel mobility if and only if all actuators have mobility in rotation in the parallel mobility direction.

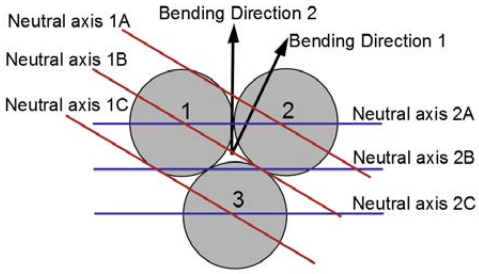

Fig. 4. Notation for actuator number, actuation directions, and neutral planes in bending for triangular triplet actuators. Shown in a top view.

For mobility directions that are screw motions, additional considerations of screw coupling need to be considered. For parallel screw mobilities that combine rotation with axial translation, 3 conditions need to be met:

1) Each actuator must either axially translate in the parallel mobility direction or have a coupled translation and rotation identical to the parallel mobility direction.
2) Each actuator must either rotate in the parallel mobility direction or have a coupled translation and rotation identical to the parallel mobility direction.
3) At least one of the actuators must have a coupled translation and rotation identical to the parallel mobility direction.

For bending motions, 3 different planes may serve as the neutral axis. Figure 4 shows the 2 fundamental bending directions for triangular triplets as well as their respective neutral axis planes. For a parallel mobility in bending the following rules must be met:

1) All actuators must have mobility in transverse bending.
2) For bending direction 1, one or more of the following must be true:
   (**i**) Actuator 2 is axially compressing and Actuator 3 is axially extending,
   (**ii**) Actuator 1 and Actuator 3 are axially extending
   (**iii**) Actuator 1 and Actuator 2 are axially compressing
3) For bending direction 2, one or more of the following must be true:
   (**i**) Actuator 1 and Actuator 2 are axially compressing
   (**ii**) Actuator 3 is axially extending

There are additional mobility sets in the direction opposite to bending directions 1 and 2 by reversing axial extension and axial compressions in each of their respective set of rules. For 120° rotation of the coordinates defining the bending direction and associated actuator numbering, the same rules will hold true. Screw motions that coordinate bending and rotation are the following:

1) The actuators must have axial translations and transverse bending according to the rules used to determine parallel mobility bending in the correct direction. These mobilities may be coupled with rotations in the parallel mobility direction.
2) Each actuator must either rotate, have a coupled transverse bend and rotation, or a coupled axial translation and rotation, with the rotation components all in the parallel mobility direction and the translations forming the correct bending direction.
3) At least one of the actuators must have either a coupled translation and rotation or a coupled transverse bending and rotation, with the rotation components all in the parallel mobility direction and the axial translations forming the correct bending direction.

B. Mobility Synthesis

The freedom of a parallel configuration is determined by finding all parallel mobilities when no actuator is undergoing volumetric expansion. The parallel actuation directions are found by setting the active actuators' mobility to the union of their active and freedom directions and setting the other actuators to their freedom mobilities. Additionally, the parallel actuation must use at least one actuation direction of an active actuator. There can be 0,1, or multiple actuation directions for the parallel configuration. The parallel mobility provides a full mapping from all actuator permutations to all parallel mobilities under all actuation combinations. An algorithm is able to parse all permutations to find all viable actuator combinations that have a desired parallel mobility.

V. Prototype Verification

To validate the motion directions predicted by the parallel kinematic synthesis, we propose experimental testing of prototypes. Five case studies spanning a wide range of actuation directions are fabricated and tested to perform a qualitative test of the predicted motion directions. The five case studies, expected motion directions, and experimental motion directions are shown in Figs. 5(a)-(c) and Figs. 6(a)-(b).

A. Fabrication and Testing Process

The actuators have a latex tube with an inner diameter of $3/8$ inches and a $1/32$ inch wall thickness (Kent Elastomer Products, Kent, OH). The fibers are made of number 10 cotton thread (Joann Fabrics), and are attached to the tube using 2 coats of rubber cement (No-Wrinkle Rubber Cement, Elmere's). Rubber end caps are also attached, followed by 2 coats of Latex rubber (Premium Liquid Latex Rubber, Tap Plastics, Oakland, CA) on each actuator, then 2 latex rubber coats to bundle multiple actuators.

The testing platform has 16 PSI high pressure and 2 PSI low pressure air manifolds with toggles at each actuator (measured with 2 Wika DO-68047-14 pressure gauges). The 2 PSI has minimal actuation effect, but inflates the actuators enough to express their constraints. The kinematics is recorded using 3-D motion capture (Vicon T-40, 8-camera, 120 fps, 4 passive markers). All single and pair permutations of actuation were tested. The coordinate data from motion capture were extracted by averaging the points in near steady state positions over a time span, then analyzed in Matlab.

The prototypes tested were actuated to produce large deformations compared to their overall size. Under such conditions, nonlinear coupling between bending and torsion affect the net coordinates of the actuator's end positions, differing from the instantaneous directions predicted by the synthesis. Thus, the experimental results are kinematically corrected based on a geometrically exact formulation [3] that uses the end coordinates and the axial twist data to predict the instantaneous direction of the bend curvature.

B. Results

The results are shown in Figs. 5(a)-(c) and Figs. 6(a)-(b) as an overlay of the predicted deformation and experimental results along the $X-Y$ plane as seen in the top view. The fiber angles tested are shown next to the motion directions. The large markers (dot, star, and triangle) indicate the estimated bend direction for each respective actuation permutation. A black dot indicates pure bending, a green triangle indicates coupled bend and counter clockwise rotation, and a blue star couples bend and clockwise rotation. The experimental bend directions are indicated with a smaller dot and a rotation arrow indicate the experimental rotation. Figure 7 shows images of the deformation of the actuator in Fig. 5(a) under all actuation permutation.

Fig. 5(a) has a combination of FREE nos. 5, 5 and 7 of Fig. 2(a) respectively in the place of actuators 1, 2 and 3. When actuator 1 alone is pressurized, the estimated bending direction is given by 1_{est} ($= \angle -30^\circ$), while the experimental direction 1_{exp} ($\approx \angle -40^\circ$). It is seen that 1_{exp} rotates counter-clockwise (dark green dot) while no rotation was

estimated in 1_{est} (black dot). Such a counter-clockwise offset is also seen for actuator 2, though to a lesser amount. The experimental directions for actuators 1, 2, and 3 all fall within $\approx \angle 10^{\circ}$ of their predicted directions. For a combination of two actuators, the methodology predicts a range of possible directions such as seen in $(1+2)_{est}$ ($\approx \angle -120^{\circ}$ to $\angle -60^{\circ}$). The experimental direction ($\approx \angle -95^{\circ}$) falls within this range. Actuators $(2+3)$ and $(1+3)$ directions fall slightly outside the range of the predicted values. The results of other fabricated prototypes have varying degrees of accuracy, as seen in Figs. 5(b)-6(b). The prototype with fiber orientation nos. 5, 12 and 19 (Fig. 6(b)) has the lowest accuracy, with the actuator rotating and bending in unpredicted directions under simultaneous actuations.

Interpretation of Results: The assumptions considered in the paper have greatly simplified the process of synthesizing parallel combination of FREEs. However, it limits the accuracy of the results in some cases. Critical analysis reveals that the predicted motion patterns involving pure bending directions with little rotation (such as FREE nos. 2 and 5) match closely. A combination of axial rotation and bending may either align closely or deviate from the kinematically corrected experimental direction.

The experiments using air pressure significantly deviates the incompressible fluid assumption. Due to this, FREEs that otherwise constrain certain deformation modes of their neighbors offer very little resistance. This is seen in Fig. 6(b) where the counter-clockwise rotation of FREE no. 12 is not constrained by FREE no. 19. Furthermore FREE no. 12 overrides the rotation of FREE no. 19 when simultaneously actuated. The other class of errors that dominate in dual actuation conditions are the elasto-kinematic effects that arise from the elastomer material properties and manufacturing inconsistencies. Furthermore, some errors in the experimental data such as effect of gravity cannot be ruled out.

VI. Conclusions

This paper aims to greatly simplify the design process of soft robots with incompressible fluids, inextensible fibers and extensible elastomers by capturing their interactions as pure geometrical relationships. These relationships in tandem with other simplifying assumptions enable a set of user-friendly design rules to (**i**) predict deformation motion directions and (**ii**) determine feasible topologies that meet a range of motion requirements for single and parallel actuator configurations. These rules do not require computationally intensive finite element analysis, thus providing a quick and easy way to scan the entire design space. However, if greater accuracy is desired, factors such as compressibility of fluids and elastomer mechanics that were thus far neglected need to be considered. Some of the main contributions of the paper are:

1) Exploration of the entire design space of FREE geometries based on their fiber orientations and identification of their individual motion behavior. This a first known effort to characterize FREEs with varied asymmetric

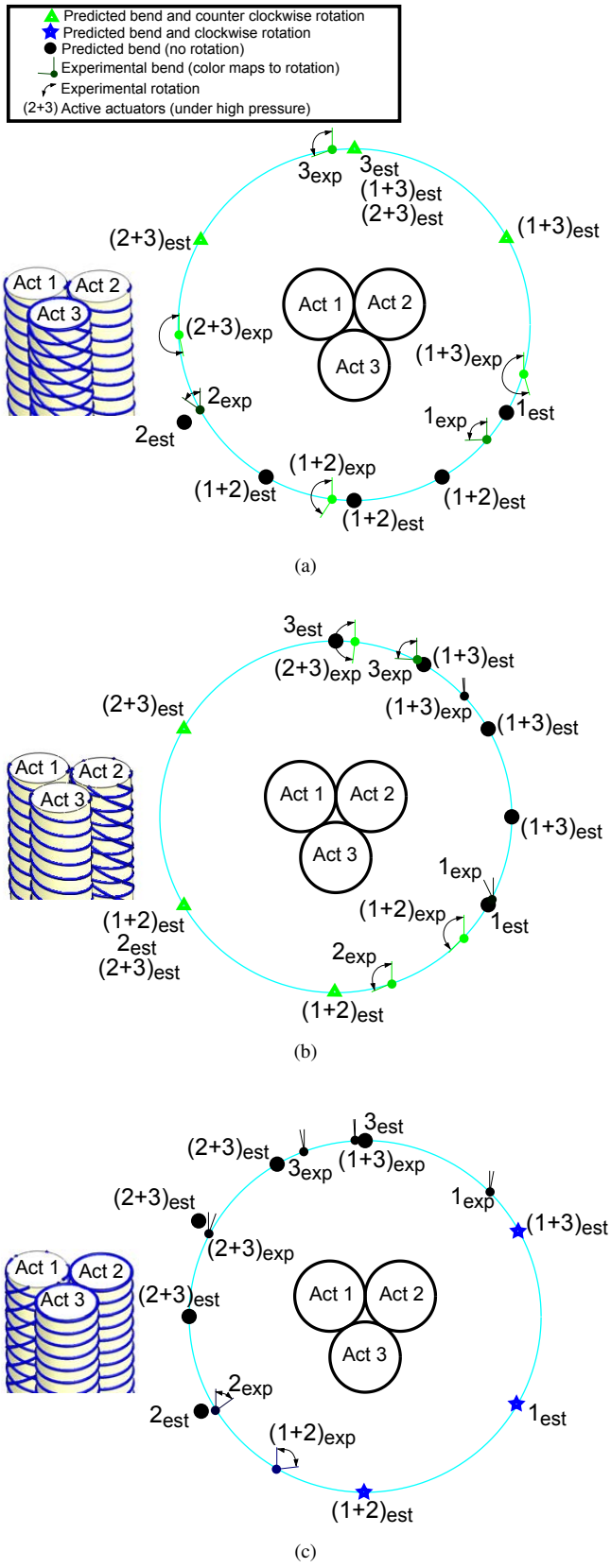

Fig. 5. Three different case studies comparing analytical predictions to kinematically-corrected experimental results. (a) FREE types 5, 5, and 7. (b) FREE types 5, 20, and 5. (c) FREE types 19, 2, and 2.

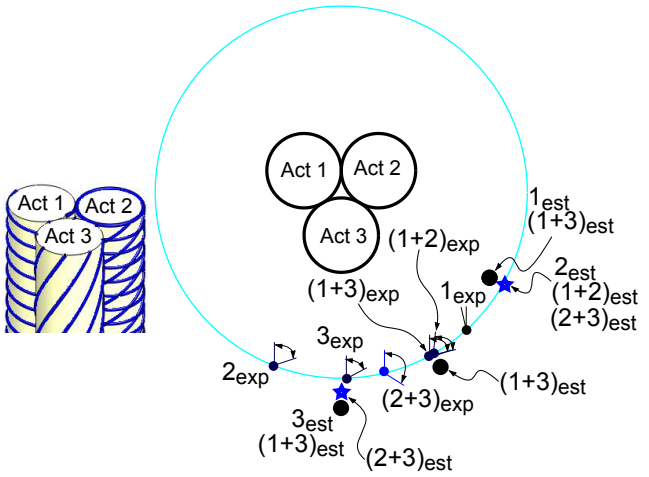

(a)

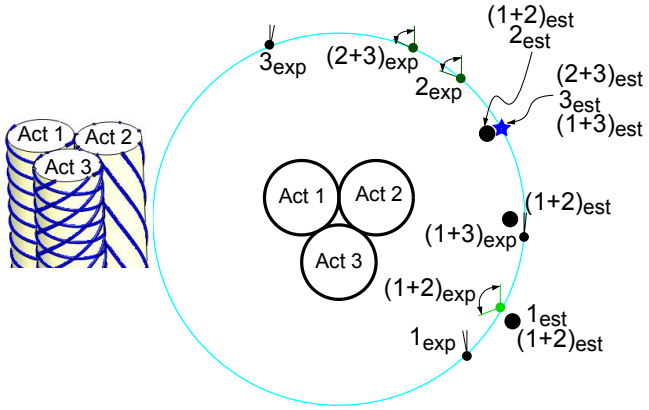

(b)

Fig. 6. Two different case studies comparing analytical predictions to kinematically-corrected exerimental results. (a) FREE types 5, 6, and 11. (b) FREE types 5, 12, and 19.

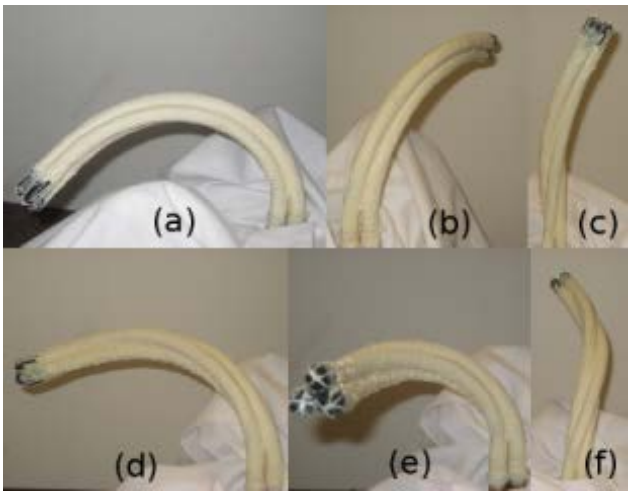

Fig. 7. Deformation of prototype with FREE types 5, 5 and 7 captured to indicate the combination of bending and screw motion. All images are looking towards the $-Y$ direction. (a) Act 1 active (b) Act 2 active (c) Act 3 active (d) Acts 1 and 2 active (e) Acts 1 and 3 active (f) Acts 2 and 3 active

fiber angles, as opposed to the symmetric arrangement of McKibben's actuators.

2) Identifying the underlying physics of combining different FREEs in parallel.
3) Proposing a first-of-its-kind systematic design methodology that determines fiber geometries of three individual FREEs that are arranged in parallel and achieve a certain motion direction.
4) Experimentally demonstrating simultaneous deformation patterns such as bending, screw motion and extension in a number of directions. This has never been previously reported for parallel soft robots.

In future work, the incompressible fluid assumption can be relaxed to yield more realistic deformation patterns. Apart from this, an analysis of series combinations of actuators may be conducted to provide a more expansive set of mobilities that may better serve practical applications. Furthermore elastomer effects must be considered in an analytical model both to evaluate the stiffness of the actuator, and to analyze the actuation forces and torques available as a function of the applied pressure.

VII. Acknowledgements

The authors would like to acknowledge the assistance of Adam Joyce. This work was supported by the National Science Foundation under NSF Award 1030887 and the Graduate Research Fellowship.

References

[1] S. Vogel, Comparative Biomechanics. Princeton, New Jersey: Princeton, 2003.
[2] G. Klute, J. Czerniecki, and B. Hannaford, Mckibben artificial muscles: pneumatic actuators with biomechanical intelligence, In *Proc. IEEE/ASME Int. Conf. on Advanced Intelligent Mechatronics*, 1999, pp. 221-226.
[3] D. Trivedi, A. Lotfi, and C. D. Rahn, C. D., Geometrically exact models for soft robotic manipulators, *IEEE Trans. on Robotics*, vol. 4, pp. 773- 780, 2008.
[4] A. De Greef, P. Lambert, and A. Delchambre, Towards flexible medical instruments: review of flexible fluidic actuators, *Precision Engineering*, Vol. 33, No. 4, pp. 311-321, Oct. 2009.
[5] D. Trivedi, C. Rahn, W. Kierb, and I. Walker, 'Soft robotics: biological inspiration, state of the art, and future research, *Applied Bionics and Biomechanics*, Vol. 5, No. 3, pp. 99 - 117, Sept. 2008.
[6] R. J. Webster III, and B. Jones, Design and kinematic modeling of constant curvature continuum robots: A review, *International Journal of Robotics Research*, Vol. 29, No. 13, pp. 1161 - 83, Nov. 2010.
[7] J. P. Merlet, Parallel Robots. New York , NY: Springer-Verlag, 2006.
[8] J. Hopkins, and M. Culpepper, Synthesis of multi-degree of freedom, parallel flexure system concepts via freedom and constraint topology (fact) part i: Principles, *Precision Engineering*, Vol. 34, No. 2, pp.259 - 70, Apr. 2010.
[9] S. Hirai, P. Cusin, H. Tanigawa, T. Masui, S. Konishi, and S. Kawamura, Qualitative synthesis of deformable cylindrical actuators through constraint topology, In *the Proc. of IEEE Int. Conf. on Intelligent Robots and Systems*, Vol. 1, pp. 197 - 201, 2000.
[10] S. Hirai, T. Masui, S. Konishi, and S. Kawamura, Prototyping pneumatic group actuators composed of multiple single-motion elastic tubes, in *the Proc. of IEEE Int. Conf. on Robotics and Automation*, Vol. 4, pp. 3807 - 3812, 2001.